Electrochimica Acta 52 (2007) 4892–4898

Cyclic voltammetry and scanning electrochemical microscopy studies of the heterogeneous electron transfer reaction of some nitrosoaromatic compounds

S. Bollo, S. Finger, J.C. Sturm, L.J. Núñez-Vergara, J.A. Squella *

Bioelectrochemistry Laboratory, Chemical and Pharmaceutical Sciences Faculty, University of Chile, P.O. Box 233, Santiago 1, Chile

Received 6 December 2006; received in revised form 28 December 2006; accepted 8 January 2007
Available online 26 January 2007

Abstract

The heterogeneous electron transfer reaction for the reduction of some nitroso aromatic derivatives in aqueous–alcoholic medium was studied on both mercury and glassy carbon electrodes (GCE) by using cyclic voltammetry (CV) and scanning electrochemical microscopy techniques (SECM).

The nitrosoaromatic derivatives followed a two-electron two-proton mechanism producing a quasi-reversible overall process. This strongly pH dependent mechanism varied from ECCE mechanism at pH < 8.5 to ECEC mechanism at pH > 8.5.

The apparent heterogeneous rate constant for the reduction of the nitroso derivatives was calculated using CV or SECM. The rate constant for the electron transfer process depends on the nature of the electrode material. The heterogeneous rate constant on the GCE is almost two orders of magnitude smaller than that on mercury electrode i.e. $(3.4 \pm 0.3) \times 10^{-3}$ cm s^{-1} on Hg and $(7.0 \pm 1.0) \times 10^{-5}$ cm s^{-1} on GCE, for the same nitroso compound and pH.

The heterogeneous rate constant values were checked by comparison between experimental and simulated cyclic voltammograms.

Keywords: Nitrosoaromatic; Heterogeneous electron transfer kinetic; Cyclic voltammetry; Scanning electrochemical microscopy

1. Introduction

1,4-Dihydropyridines (1,4-DHP) calcium antagonists, from the nifedipine family, have been broadly studied because of their relevant therapeutic uses [1]. Several of these compounds are sensitive to light, and during light exposure are easily converted to substances with less potency as calcium antagonist compared with their parent compound [2–4]. Nifedipine is extremely light sensitive and several studies have shown that the nitrosopyridine derivative is the main photodegradation product of nifedipine [5–7]. Further studies have shown that all the *ortho*-nitro substituted 1,4-DHP are far more sensitive to light than the meta-nitro substituted derivatives. In the case of the *ortho*-nitro substituted, they are unstable to both daylight and UV irradiation, the nitroso derivative being the main degradation product from artificial daylight irradiation [8]. Considering the importance of these nitroso derivatives as potential biodegradation products, a novel series of C-4 nitrosophenyl 1,4-dihydropyridines has been recently synthesized in order to study its redox pattern [9].

The reduction of nitrosoaromatic compounds has gained relatively little attention when compared with the corresponding nitroaromatic derivatives. The studies of nitrosoaromatic compounds are usually restricted almost exclusively to nitrosobenzene [10–14]. There is a report, however, on the electrochemical behavior of the photodegradation product of nifedipine, i.e., 2,6-dimethyl-4-(2-nitrosophenyl)-3,5-pyridinecarboxylic acid dimethyl esther [7]. More recently [15], an electrochemical study was carried out of the reduction of a series of six C-4 nitrosophenyl 1,4-dihydropyridines and a comparison with the parent nitrophenyl derivatives. In that study, a 2-electron 2-proton mechanism was found for the electroreduction of the nitrosophenyl derivatives according to the following overall reaction:

$$\text{R–NO} + 2e^- + 2H^+ \rightarrow \text{RNHOH} \quad (1)$$

* Corresponding author. Fax: +56 2 7371241.
E-mail address: asquella@ciq.uchile.cl (J.A. Squella).

doi:10.1016/j.electacta.2007.01.003

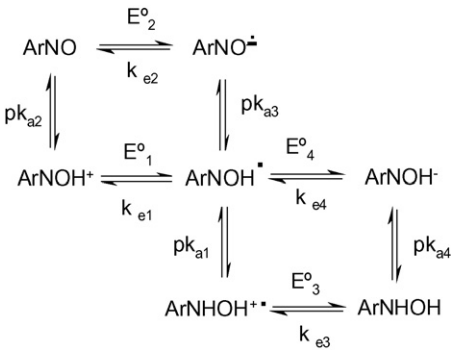

Scheme 1.

Furthermore, a quasi-reversible electron transfer for the overall mechanism was determined from the changes in ΔE_p values with the sweep rate. In addition, a change on the mechanism from pH 7 to 9 was determined from the E_p–pH dependence. All these results are in accordance with those reported by Laviron et al. [10], who proposed the following cubic overall mechanism (Scheme 1) for nitrosobenzene electroreduction.

The current study deepens in the dilucidation of the electrode kinetics of the nitrosoaromatic derivatives. Specifically this work is focused on the determination of the heterogeneous electron transfer rate constants (k^0) for the reduction of three nitrosophenyl derivatives. On the other hand, the scanning electrochemical microscopy (SECM) proved to be advantageous over conventional electrochemical methods to obtain small rate constants [16–21]. Thus, we used cyclic voltammetry and scanning electrochemical microscopy to obtain a broader range for studying k^0 in both Hg and glassy carbon electrodes.

2. Experimental

2.1. Compounds (Fig. 1)

The compounds were synthesized in our laboratory [9], and correspond to: 4-(3-nitrosophenyl)-2,6-dimethyl-3,5-dimethoxycarbonyl-1,4-dihydropyridine (*m*-NO–Me); 4-(3-nitrosophenyl)-2,6-dimethyl-3,5-diethoxycarbonyl-1,4-dihydropyridine (*m*-NO–Et); 4-(3-nitrosophenyl)-2,6-dimethyl-3,5-diisopropil-oxycarbonyl-1,4-dihydropyridine (*m*-NO–iPr).

2.2. Solutions

The working solutions for cyclic voltammetry and SECM experiments were prepared to obtain final concentrations of 0.5 or 1 mM of each nitrosoaromatic derivative. A mixture of Britton–Robinson 0.04 M, KNO_3 0.2 M/EtOH: 1/1 was used as reaction medium. The pH was adjusted with little aliquots of concentrated NaOH or HCl, respectively. All the reagents were of analytical grade.

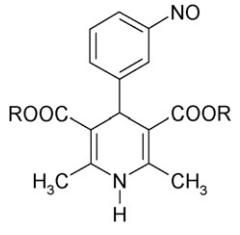

R	Compound
-CH_3	m-NO-Me
-CH_2-CH_3	m-NO-Et
-CH-(CH_3)$_2$	m-NO-iPr

Fig. 1. Molecular structure of the 4-(3-nitrosophenyl)-2,6-dimethyl-3,5-dialcoxycarbonyl-1,4-dihydropyridine derivatives.

2.3. Methods

2.3.1. Cyclic voltammetry

Experiments were carried out in a BAS 100 W assembly (Bioanalytical System, USA). All cyclic voltammograms were recorded at a constant temperature of 20 ± 0.1 °C and the solutions were purged with pure nitrogen for 10 min before the voltammetric runs.

A BAS hanging mercury drop electrode (HMDE) with a drop surface of 1.90 mm^2 (VC) and a 3 mm diameter glassy carbon disc were used as working electrodes. A platinum wire was used as a counter electrode. All potentials were measured against an Ag/AgCl reference electrode. The solution resistance was compensated, and a stabilizing capacitor was used (0.1–1 μF) [22].

The heterogeneous rate constant k^0 for the ET reaction was obtained using the methodology described by Nicholson [23]. Briefly, this method relates the heterogeneous rate constant with the peak potential separation (ΔE_p) through a working curve and the dimensionless kinetic parameter Ψ. Ψ is obtained from the $n\Delta E_p$ versus log Ψ plot, for each sweep rate (ν), using a linearization of the Nicholson approach informed by Leddy et al. [24]. Finally, the obtained Ψ value and its corresponding sweep rate (ν), permitted to calculate k^0 using:

$$\psi = \frac{\gamma^{\alpha} K}{(\pi a D_O)^{1/2}} \quad (2)$$

where $a = nF\nu/RT$, $\gamma = (D_O/D_R)^{1/2}$, $\gamma^{\alpha} = (D_O/D_R)^{\alpha/2} \approx 1$, for $D_O \approx D_R$ and D_O and D_R stand for the diffusion coefficient of the oxidized and reduced species, n the number of electrons transferred, R corresponds to the gas constant, F the Faraday constant, T the temperature, α the transfer coefficient and ν is the sweep rate.

2.3.2. Scanning electrochemical microscopy

The SECM experiments were carried out with a CHI 900 setup (CH Instruments Inc., USA). A nominally 10 μm diameter Carbon Fiber electrode served as the SECM tip. A 3 mm diameter glassy carbon disc electrode was used as the SECM substrate. A 0.5 mm diameter Pt wire and an Ag|AgCl|KCl saturated electrode were used as counter and reference electrodes, respectively. Before each experiment the tip and the substrate were polished with 0.3 and 0.05 μm alumina, and then rinsed with water. All the experiments were performed at controlled temperature (20 ± 1 °C). The feedback mode is the main quantitative operation mode of SECM. When both the tip is far from the substrate, and a potential permitting the occurrence of the redox process is applied, the steady-state current, $i_{T,\infty}$, is given by

$$i_{T,\infty} = 4nFDCa \quad (3)$$

where F is the Faraday constant, n the number of electrons transferred in the tip reaction, D the diffusion coefficient of electroactive specie, C the bulk concentration of the specie and "a" is the tip radius. When the substrate is conductive, a higher tip current is observed ($i_T > i_{T,\infty}$) when the tip is closer to substrate, then a positive feedback takes place. Whereas the substrate is insulating, a lower tip current is observed ($i_T < i_{T,\infty}$) when the tip is closer to the substrate, which means that a negative feedback takes place. SECM results are presented in the dimensionless form I_T (L) versus L, where the experimental feedback current was normalized by steady-state current, $i_{T,\infty}$, i.e., $I_T(L) = i_T/i_{T,\infty}$ and L is d/a.

The heterogeneous rate constant k^0 for the ET reaction can be obtained from fitting SECM experimental current (I_T)–distance (d) curve (or approach curve) to the theoretical value. The experimental I_T–d curve was recorded while the tip was approaching the substrate surface at a speed of 0.1 μm s^{-1}. A sufficiently negative potential (−1.0 V) was applied to the tip so that the nitroso compound was reduced at diffusion-limited rate. For each current–distance curve, the substrate was polarized at different potential, between 0.0 and 0.7 V prior and during data acquisition. After the experimental data were obtained, a theoretical fitting equation was used [16–21], and the best fit of K_b was obtained, where K_b corresponds to the dimensionless kinetic parameter ($K_b = ak_{b,s}/D$). The rate constant for oxidation ($k_{b,s}$) at the substrate is given by the following equation obtained from the well-known Butler–Volmer equation:

$$K_b = \left(\frac{ak^0}{D}\right) \exp\left[\frac{(1-\alpha)nF(E-E^{0'})}{RT}\right] \quad (4)$$

where k^0 is the heterogeneous rate constant, E the electrode potential, $E^{0'}$ the formal potential, α the transfer coefficient, n the number of electrons transferred per redox event, F the Faraday constant, R the gas constant, T the absolute temperature, D the diffusion coefficient of the electroactive specie and "a" is the tip radius. The subscripts indicate the substrate process. Thus, a plot of Ln $K_{b,s}$ versus ($E_s - E^{0'}$) will give α and k^0.

The diffusion coefficient of each compound was determined from the steady state diffusion limiting current, $i_{T,\infty}$, obtained from the approach curves and using Eq. (3). For the determination of the diffusion coefficient a value of $n = 2$ was used for the number of electrons involved in the reaction.

2.3.3. Digital simulations

Simulated CV curves were obtained using software DIGISIM® 2.1CV simulator for Windows. The simulated curves proposed mechanism was simulated according the experimental and calculated values of peak potentials and heterogeneous rate constants.

3. Results and discussion

Recently a comprehensive study of the electrochemical reduction in protic media of C-4 nitrophenyl 1,4-DHPs and their corresponding nitrosophenyl 1,4-DHPs was published [15]. That electrochemical study concluded that the overall electroreduction mechanism of nitroso derivatives followed a two-electrons two-protons mechanism (Eq. (1)) producing a quasi-reversible overall process, but no calculations were done of the heterogeneous electron transfer constants.

According Laviron [10], the protonation reactions are fast, i.e. in equilibrium, in the used protic medium, then, the reduction mechanism represented in the above Scheme 1 can be simplified to two-electron consecutive reactions:

$$B \underset{k_1^0}{\overset{E_1}{\rightleftarrows}} B^{-1} \underset{k_2^0}{\overset{E_2}{\rightleftarrows}} B^{-2}$$

Then, the heterogeneous rate constant determined for this system would be an apparent constant (k^0_{app}) that will depend on the individual heterogeneous rate constants (k_1^0 and k_2^0), on the standard redox potential (E_1^0 and E_2^0) and on pK_a.

3.1. Cyclic voltammetry

Using a HMDE, the cyclic voltammetric experiments reveal that the electroreduction of the nitroso derivatives displayed only one reduction signal in the forward sweep with the corresponding anodic signal in the reverse sweep in all the pH range studied (7–12) (Fig. 2). This signal is in concordance with the well-known two-electron, two-proton reduction of nitroso moiety to generate the corresponding hydroxylamine derivative. For three compounds the signals shifted to more cathodic potential as the pH increased, no differences were found in the peak potential values between them.

The relationship between peak current and sweep rate (log I_p versus log ν plot) showed that the slopes were very close to 0.5 in all the pH range under study. Therefore the electrodic process has a diffusion control without any adsorption phenomenon complicating the electron transfer [25]. Thus, an accurate determination can be carried out of the electron transfer rate of the process.

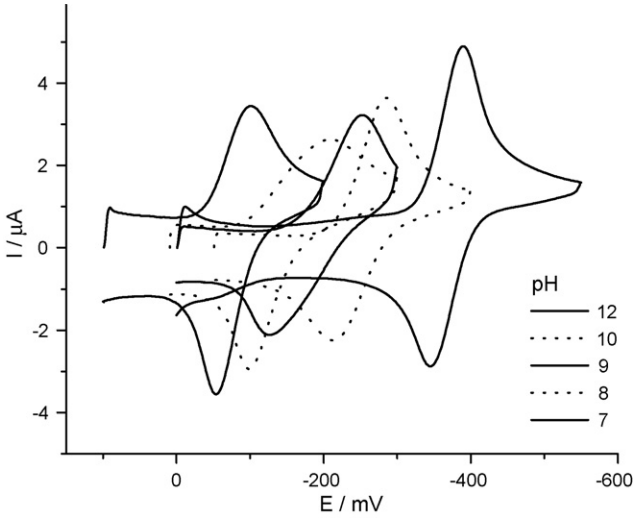

Fig. 2. Cyclic voltammograms at HMDE of 0.5 mM *m*-NO–iPr in Britton–Robinson 0.04 M, KNO_3 0.2 M/EtOH: 1/1 at different pHs. Sweep rate 5 V/s.

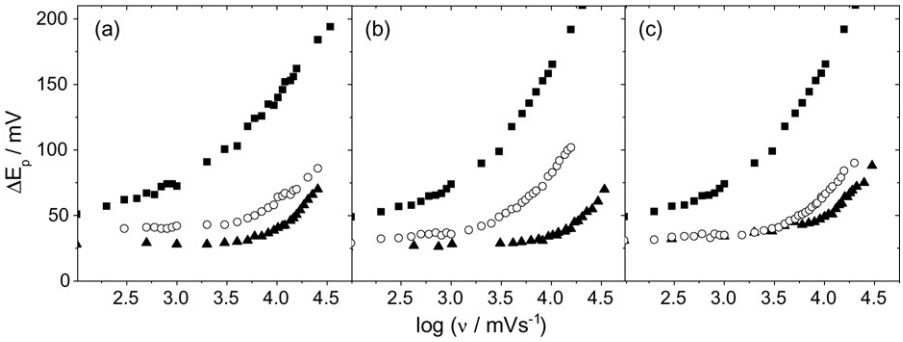

Fig. 3. Cyclic voltammetric ΔE_p dependence with the log of sweep rate at pHs 7 (◯), 9 (□) and 12 (ρ) for: (a) *m*-NO–Me, (b) *m*-NO–Et and (c) *m*-NO–iPr. Britton–Robinson 0.04 M, KNO_3 0.2 M/EtOH: 1/1.

In Fig. 3, the dependence is shown of ΔE_p with the sweep rate at pHs 7, 9 and 12 for each compound. At every pH and in all compounds, there is a clear increase of the ΔE_p value as the sweep rate is increased, revealing that electron transfer kinetics has a quasi-reversible behavior ($\Delta E_p > 59/n$). Nevertheless, when the effect of the pH medium is evaluated, a special response is observed, since between pH 8 and 10 the cyclic voltammetric signals are broader and the peak potential difference (ΔE_p) is greater than that observed at pH 7 and 12. A maximum value in the ΔE_p value is around pH 9 for all compounds.

In order to elucidate the nature of this electron transfer mechanistic change of the nitroso derivative, the apparent heterogeneous rate constants k^0_{app}, was calculated for every pH. For this purpose, we used the methodology described by Nicholson in 1965 [23] and adapted by Leddy in 1995 [24]. The Nicholson's methodology can be applied to systems in which homogeneous chemical reactions precede or follow electron transfer provided such reactions are either rapid or slow compared to the rate constant for electron transfer. This methodology is based on the change of ΔE_p values with sweep rate in the cyclic voltammetric experiments, as detailed in the experimental section. The constants are presented in Table 1 showing a strong influence of pH on electron transfer kinetics. As observed from the results, at pH 7 and 12 the values are several times higher than those at 8, 9 and 10. On the other hand, from the plot between K^0_{app} and pH (Fig. 4A) we can state that all the nitroso derivatives have the same tendency, discarding any possible influence of the substituents on the 1,4-DHP moiety in spite of their particular difference in volume.

From this Fig. 4A, it is also evident that the minimum value of k^0_{app} is at pH 8.5 where the electron transfer is the slowest, i.e., the system is more irreversible compared with the others pHs. This behavior agrees with that previously described [15] using differential pulse polarography. In that study, a break in the dependence of the peak potential with the pH of the medium was clearly observed at pH 9. Both results would indicate a change in the mechanism of the electron-proton transfer.

On the other hand, Laviron et al. [10] reported for nitrosobenzene that a minimum at pH 8 is present in the $\log k^0$ vs pH plot, with slopes of −0.5 and 0.5 before and after this value. According to Laviron, a change in the mechanism is observed when the slope of the $\log k^0$ versus pH plot swap from negative to positive value. In particular, below the pH of change, an ECCE ($e^-/H^+/H^+/e^-$) mechanism is occurring in the reduction of nitrosobenzene to hydroxylaminebenzene, whereas above this pH value the mechanism changed to ECEC ($e^-/H^+/e^-/H^+$). In our case this change in the slope is produced at pH 8.5 (Fig. 4B–D). Furthermore, the null influence of the substituents in the 1,4-DHP ring can be concluded on the electroreduction mechanism.

In order to study the influence of the electronic conductor nature on the heterogeneous rate constants we also tried with a glassy carbon electrode. Consequently we carried out cyclic voltammograms using the glassy carbon electrode as the working electrode. In this case, one reduction signal was also observed for the electroreduction of the nitroso compounds, however the redox couples showed greater values of ΔE_p (∼500 mV), showing that the electron transfer is still slower than that observed at HMDE (data not shown). Due to these values the cyclic voltammetry methodology of Nicholson [23] can not be used, because the range in which the theory operated is $61 < \Delta E_p < 212$ mV. To solve this impasse we decided to use the SECM methodology to obtain the apparent heterogeneous rate constant on the glassy carbon electrode.

Table 1
Cyclic voltammetric determined apparent heterogeneous rate constants for each compound at HMDE and different pH

	K^0_{app} ($\times 10^{-3}$ cm s^{-1})				
	7	8	9	10	11
m-NO–Me	18.0 ± 0.3	5.3 ± 1.0	3.1 ± 0.3	–	41.0 ± 1.3
m-NO–Et	20.1 ± 0.6	2.9 ± 0.3	3.3 ± 0.5	8.9 ± 1.9	42.0 ± 1.4
m-NO–iPr	15.0 ± 0.8	4.7 ± 0.6	3.4 ± 0.3	8.4 ± 1.0	41.0 ± 0.8

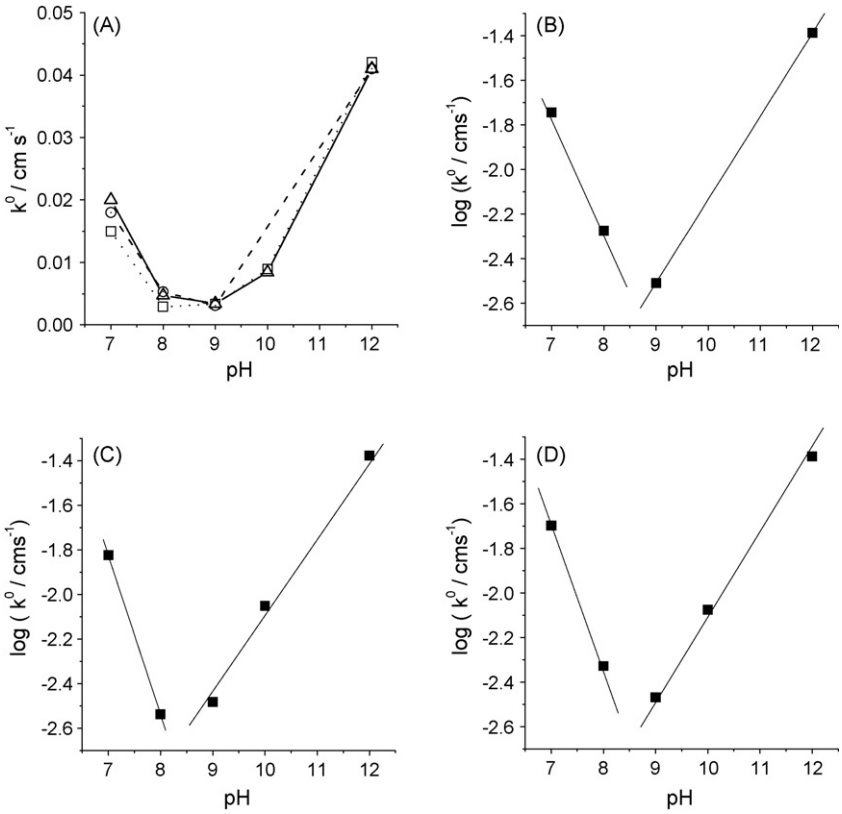

Fig. 4. Heterogeneous rate constant determined at mercury electrode dependence with pH. (A) Comparison of k versus pH plot for: *m*-NO–Me (◯), *m*-NO–Et (□)) and *m*-NO–iPr (ρ) and log *k* vs. pH for each independent compound: (B) *m*-NO–Me, (C) *m*-NO–Et and (D) *m*-NO–iPr.

3.2. SECM

SECM permitted to study slower electron transfers than cyclic voltammetry since microelectrodes avoid problems as uncompensated IR drop in solution. Thus the SECM can be used for quantitative determination of both slow and rapid heterogeneous ET rate constants at microscopic domains [26].

Cyclic voltammetric experiments were conducted using a 10 μm carbon fiber tip electrode to determine the steady state current for the reduction of each compound (data not shown). From these values and using Eq. (3), the corresponding diffusion coefficients were determined. The values obtained were: 1.4, 1.5 and 1.4×10^{-6} cm^2 s^{-1} for *m*-NO–Me, *m*-NO–Et and *m*-NO–iPr, respectively. In the previous paper of Laviron [10] a value of 4.25×10^{-6} cm^2 s^{-1} was polarographically determined for nitrosobenzene in aqueous medium.

The apparent heterogeneous rate constant k^0_{app} was calculated by fitting the SECM experimental current (I_T)–distance (d) curve to the theoretical values. Fig. 5A shows the schematic representation of the SECM experiments, where a series of approach curves was conducted between the tip and substrate. At the tip, the reduction of the nitroso compound to form the corresponding hydroxylamine is produced, while at the substrate, only when the electrodes are very close, the applied potential permits the regeneration of the parent nitroso compound, i.e., a feedback between both electrodes is taking place. But, in the quasi-reversible situation, when the tip approaches the substrate, the tip current response to distance depends only upon the k_b value of the reverse reaction on the substrate, GCE in our case. Since the rate constant for the oxidation of the hydroxylamine (k_b) at the substrate is given by the Butler–Volmer equation (see methods), a change in overpotential, η, (while keeping constant the values all the other parameters) will influence the resulting feedback current.

Fig. 5B, shows the experimental (squares) and simulated (solid lines) approach curves for *m*-NO–Et at pH 9 at different substrate potentials (0.5, 0.4, 0.3 and 0.25 V); the GCE cyclic voltammogram for the same conditions is presented (inset Fig. 5B). These results clearly show the difference between the microscopic approach via SECM experiments versus the macroscopic approach via CV experiments. In CV measurements, only one CV curve was obtained and the sweep rate of the experiment must be changed for the determination of the heterogeneous rate constant with the uncompensated IR drop-associated problems. On the other hand, SECM experiments permitted to obtain different approach curves with different feedback currents depending on the substrate potential applied. Furthermore, the approach curves showed behaviors ranging from a totally positive feedback current (curve a) at sufficiently high η to a more negative feedback current (curve d) when η is low, but in the intermediate state the situation is rather different showing a tip current increase and later decay.

Fig. 6 shows the approach curves at constant η for *m*-NO–iPr at pHs 8.0, 9.0, 10.0 and 11.0. This figure shows a notorious change in the shape of the curves, indicating a change in the rate of the electron transfer reaction k^0_{app} when the pH was changed.

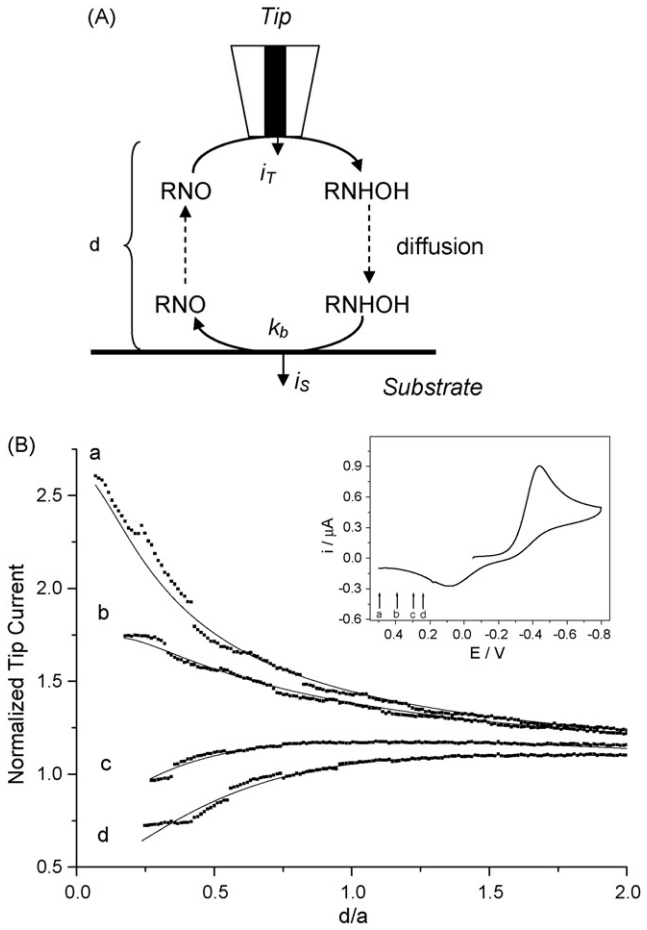

Fig. 5. (A) Schematic representation of the SECM experiment; (B) experimental (squares) and simulated (solid lines) approach curves for *m*-NO–Et, pH 9, obtained at different substrate applied potentials, curves: $a = 0.5$, $b = 0.4$, $c = 0.3$ and $d = 0.25$ V. Inset: cyclic voltammograms at GCE of 0.5 mM *m*-NO–Et at pH 9. Sweep rate 5 V/s Britton–Robinson 0.04 M, KNO_3 0.2 M/EtOH: 1/1.

The more insulating curves were obtained for the curves at pHs 8 and 9.

After the approach experiments, the experimental I_T–d curves were fitted with the theoretical values to estimate the corresponding K_b value. Finally from the plot Ln K_b versus η and according to Eq. (4) the k^0_{app} value for each pH can be determined from the intercept of the curve (data not shown).

Table 2 shows the corresponding values calculated for each compound, which are significantly lower than those with the mercury electrode (i.e. 10^{-5} versus 10^{-3} cm s^{-1}), indicating that the potential energy barrier height has a larger value for GCE compared to the mercury electrode, since k^0_{app} is inversely proportional to the barrier maximum [27]. This result can be explained on the basis of the work function of the electrodic

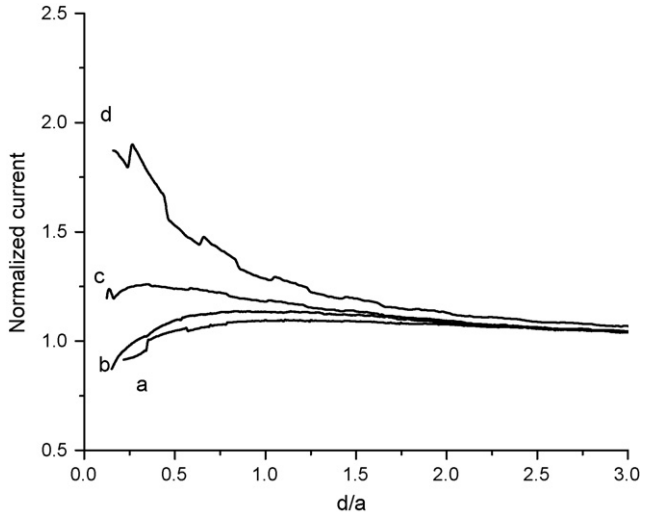

Fig. 6. Experimental approaches curves obtained at a constant overpotential (0.5 V) and at different pHs: 8 (a), 9 (b), 10 (c) and 11 (d), for 0.5 mM *m*-NO–iPr in Britton–Robinson 0.04 M, KNO_3 0.2 M/EtOH: 1/1. Substrate electrode: GCE.

phase wherein smaller values of work function favor electron transfer easily. In this case the work function of the mercury is obviously lower than that of the GCE.

Furthermore, the fact that heterogeneous electron transfer rates are higher at mercury than at GCE is well known [28,29].

3.3. Digital simulations

In order to check the calculated k^0_{app}, and the proposed redox mechanisms, digital simulations were carried out through the use of the CV simulation Digisim® software. The uses of this simulator to study nitrosocompounds have been previously reported [30]. To achieve an adequate simulation, we used the Laviron's mechanism, i.e., two-electron consecutive reactions and the assumption that the protonation reactions are fast, i.e. in equilibrium, since we are using a protic medium.

Fig. 7 shows the experimental and simulated CVs for both, HMDE and GCE electrodes, at each pH for *m*-NO–DHP. These results clearly show an agreement between the calculated constant and the simulated ones and confirm a very fast protonation, non interfering with the electrodic process. Securely the observed differences between experiment and calculated curves are due to a little more complex behaviour than the assumed in this paper. Probably the more complex behaviour is related to adsorption or some other coupled chemical reaction such as nitroso with hydroxylamine derivatives but at the current level of our experiments any suggestion in this way would be rather speculative.

Table 2
SECM determined apparent heterogeneous rate constants for nitroso derivatives at glassy carbon electrode and different pH

	K^0_{app} ($\times 10^{-5}$ cm s^{-1})				
	7	8	9	10	11
m-NO–Et	11.0 ± 0.8	3.8 ± 0.5	6.2 ± 0.9	18.0 ± 1.2	38.0 ± 2.6
m-NO–iPr	15.0 ± 0.9	3.6 ± 0.4	7.0 ± 1.0	17.0 ± 1.8	39.1 ± 2.7

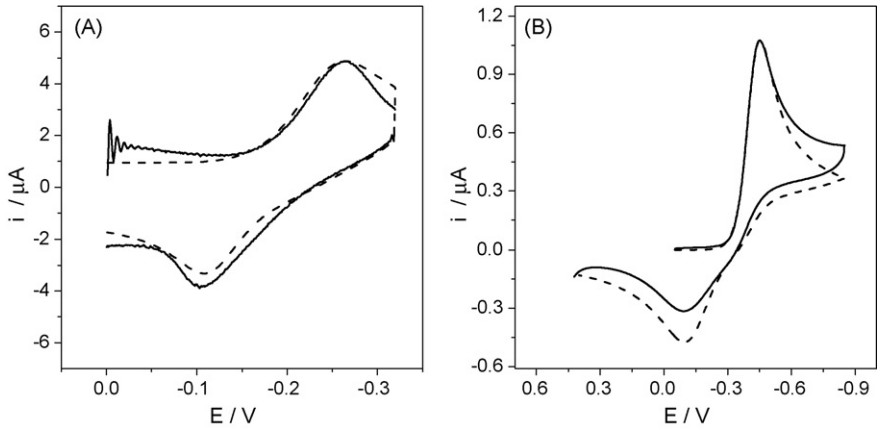

Fig. 7. Experimental (solid) and simulated (dashed) cyclic voltammograms of *m*-NO–DHP in Britton–Robinson 0.04 M, KNO_3 0.2 M/EtOH: 1/1 at (A) HMDE pH 9 at 15 V/s, k^0_{app} 3.1×10^{-3} cm s^{-1} and (B) GCE pH 11 at 0.5 V/s k^0_{app} 3.5×10^{-4} cm s^{-1}.

4. Conclusions

Summing up, the rate of the electron transfer reactions is strongly dependent on both pH and electrode materials, the reduction on GCE being almost two magnitude orders lower than the same reduction on the mercury electrode, which means that the potential energy barrier has a larger value for GCE compared with mercury. This is probably due to the fact that the work function for mercury electrode is lower than that of GCE.

On the other hand, independent of the electrode material, a quasi-reversible reduction mechanism was observed for the studied nitrosoaromatic derivatives with a strongly pH dependent change from an ECCE mechanism at pH < 8.5 to an ECEC mechanism at pH > 8.5, i.e., they follow a similar mechanism to those already reported in literature. Furthermore, the apparent heterogeneous rate constant was obtained using both, cyclic voltammetric and SECM approaches. While the CV approach was selected for higher rate constants on the mercury electrode, SECM was used for lower rate constants on GCE.

This study demonstrates that SECM can be a useful alternative technique for determination of heterogeneous rate constant of processes sufficiently slow to be determined by cyclic voltammetry. Consequently, this is the first time that SECM is used to determine the heterogeneous rate constant of nitrosoaromatic compounds.

Acknowledgements

Financial support from FONDECYT (Grant No. 8000016) and University of Chile is gratefully acknowledged. We are also grateful to professor Claudio Telha for the English revision.

References

[1] Drug Future 13 (3) (1988) 207.
[2] S. Ebel, H. Schütz, A. Hortnitschek, Arzneim.-Forsch. (Drug Res.) 28 (1978) 2188.
[3] M. Sanguinetti, Kass.F R., Biophys. J. 45 (1984) 873.
[4] M. Sanguinetti, R. Kass, Biophys. J. 45 (1984) 873.
[5] P. Pietta, A. Rava, P. Biondi, J. Chromatogr. 210 (1981) 516.
[6] P. Jakobsen, O. Lederballe, O. Mikkelsen, J. Chromatogr. 162 (1979) 81.
[7] L.J. Núñez-Vergara, S. Bollo, J. Fuentealba, J.C. Sturm, J.A. Squella, Pharm. Res. 19 (4) (2002) 522.
[8] J.A. Squella, L.J. Núñez-Vergara, Electrochemistry of 1,4 dihydropyridine calcium channel antagonist compounds, in: H. Fernandez, M.A. Zón (Eds.), Recent Developments and Applications of Electroanalytical Chemistry, Research Signpost, India, 2002, p. 107.
[9] I.P. Santander, L.J. Núñez-Vergara, J.A. Squella, P.A. Navarrete-Encina, Synthesis 18 (2003) 2781.
[10] E. Laviron, A. Vallat, R. Meunier-Prest, J. Electroanal. Chem. 379 (1994) 427.
[11] W. Kemula, R. Sioda, J. Electroanal. Chem. 6 (1963) 183.
[12] E. Steudel, J. Posdorfer, R. Schindler, Electrochim. Acta 40 (1995) 1587.
[13] M. Asirvatham, D. Hawley, J. Electroanal. Chem. 57 (1974) 179.
[14] C. Lamoureux, C. Moinet.Bull, Soc. Chim. Fr. 1 (1988) 59.
[15] L.J. Núñez-Vergara, P. Santander, P.A. Navarrete-Encina, J.A. Squella, J. Electroanal. Chem. 580 (2005) 135.
[16] A.L. Barker, P.R. Unwin, S. Amemiya, J.F. Zhou, A.J. Bard, J. Phys. Chem. B 103 (1999) 7260.
[17] J.B Allen, V.M Michael, R.U Patrick, 0.W David, J Phys Chem. 96 (1992) 1861.
[18] A.J. Tsionsky, M.V. Bard, Mirkin, J. Phys. Chem. 100 (1996) 17881.
[19] J. Zhang, P.R. Unwin, J. Phys. Chem. B 104 (2000) 2341.
[20] J. Zhang, C.J. Slevin, P.R. Unwin, Chem. Commun. (1999) 1501.
[21] C.J. Slevin, P.R. Unwin, Langmuir 15 (1999) 7361.
[22] P. He, L.R. Faulkner, Anal. Chem. 58 (1986) 517.
[23] R.S. Nicholson, Anal. Chem. 37 (1965) 1351.
[24] H.J. Pad, J. Leddy, Anal. Chem. 67 (1995) 1661.
[25] D.K. Gosser Jr., Cyclic Voltammetry: Simulation and Analysis of Reaction Mechanisms, VCH Publishers, New York, 1993, p. 43.
[26] K. Borgwarth, J. Heinze, Heterogeneous electron-transfer reactions, in: A.J. Bard, M.V. Mirkin (Eds.), Scanning Electrochemical microscopy, Marcel Dekker Inc., New York, 2001, p. 201.
[27] N.K. Bhatti, M.S. Subhani, A.Y. Khan, R. Qureshi, A. Rahman, Turk. J. Chem. 29 (2005) 659.
[28] E. Laviron, L. Roullier, J. Electroanal. Chem. 157 (1983) 7.
[29] T.W. Rosanske, D.H. Evans, J. Electroanal. Chem. 72 (1976) 277.
[30] L.J. Nuñez-Vergara, M. Bonta, J.C. Sturm, P.A. Navarrete, S. Bollo, J.A. Squella, J. Electroanal. Chem. 506 (2001) 48.